For submission to *Dalton Trans.*

New dinuclear ruthenium arene complexes containing thiosemicarbazone ligands: synthesis, structure and cytotoxic studies

Wei Su,[a] Zhaofeng Tang,[a] Peiyuan Li,*[,b] Gufeng Wang,[c] Qi Xiao,[a] Yuchun Li,[a] Shan Huang,[a] Yunqiong Gu,[a] Zefeng Lai,[d] Yuexing Zhang[e]

[a] Key Laboratory of Environment Change and Resources Use in Beibu Gulf (Guangxi Teachers Education University), Ministry of Education, China

[b] College of Pharmacy, Guangxi University of Chinese Medicine, Nanning, China. E-mail: lipearpear@163.com

[c] Department of Chemistry, North Carolina State University, Raleigh, North Carolina 27695, United States.

[d] Department of Pharmacology, Guangxi Medicinal University, Nanning 530021, China.

[e] Department of Chemistry, Hubei University, Wuhan 430062, China.

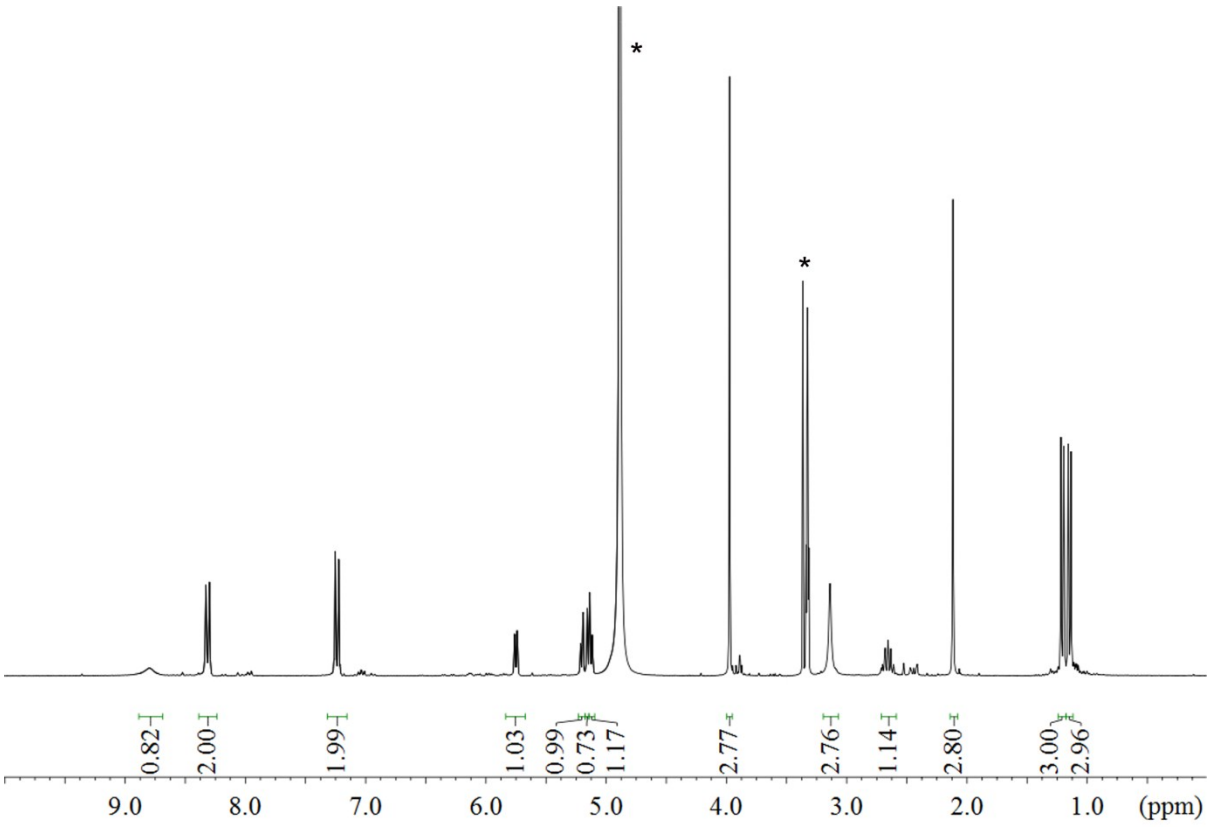

Fig. S1.[1]H NMR spectra of **1**.

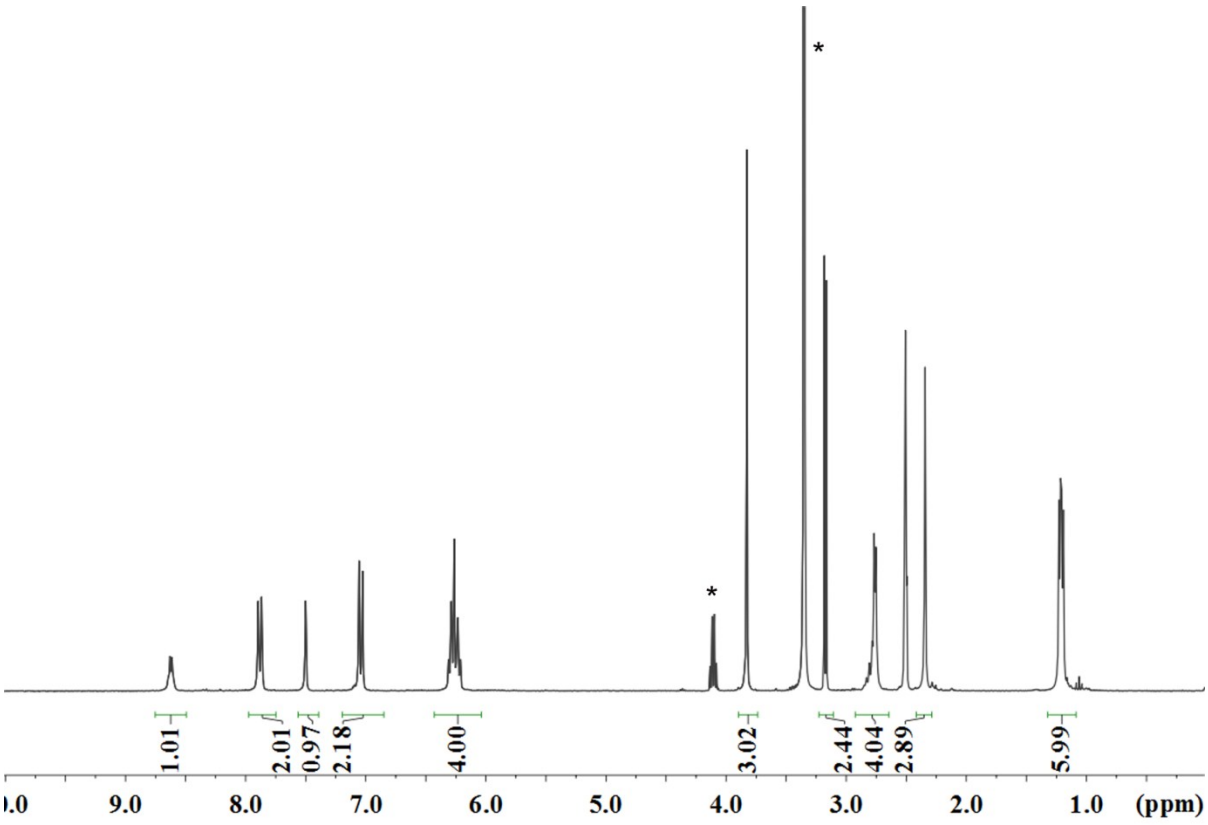

Fig. S2.^{1}H NMR spectra of **9**.

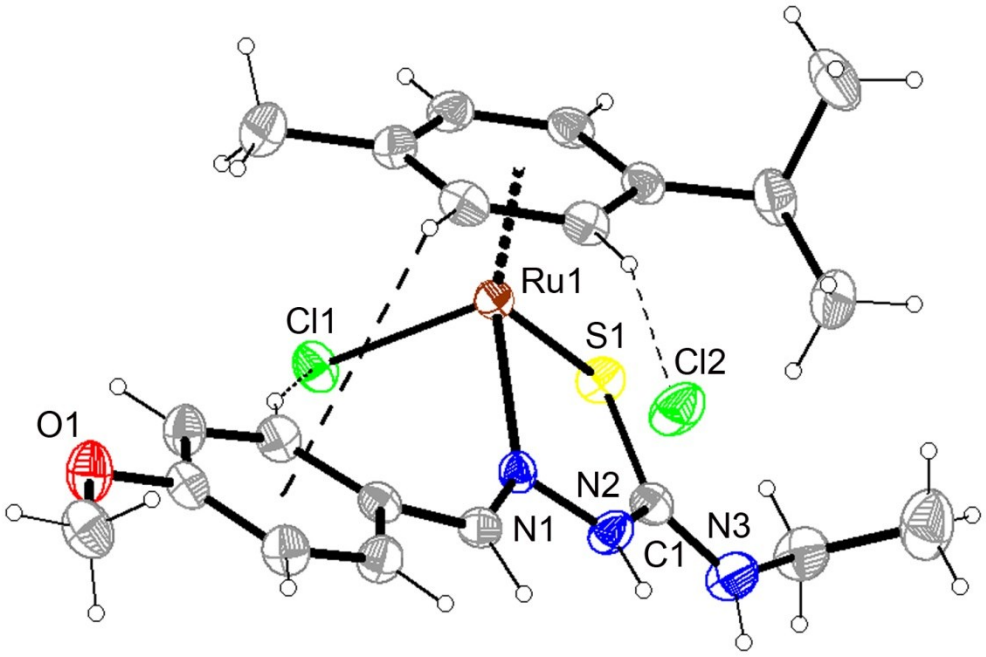

Fig. S3. ORTEP plots of **2**.

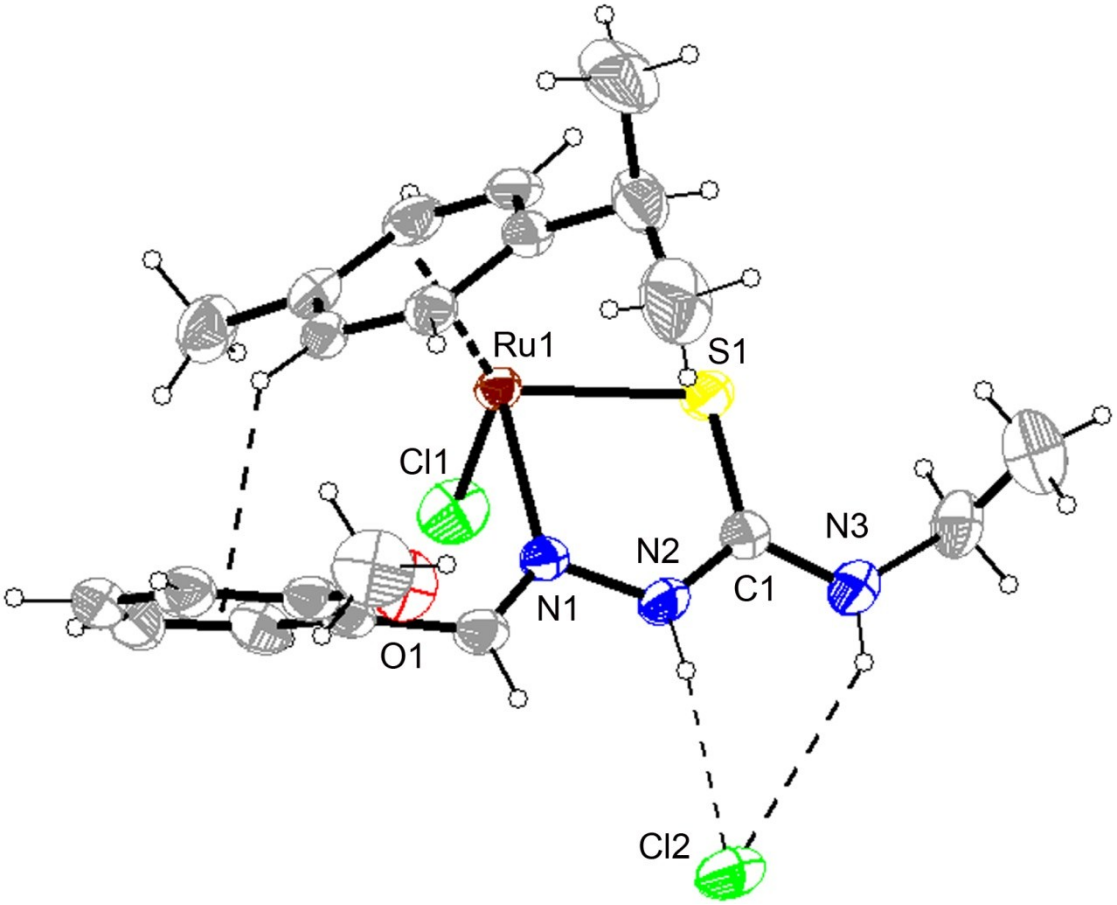

Fig. S4. ORTEP plots of **6**, the solvent molecules have been omitted for clarity.

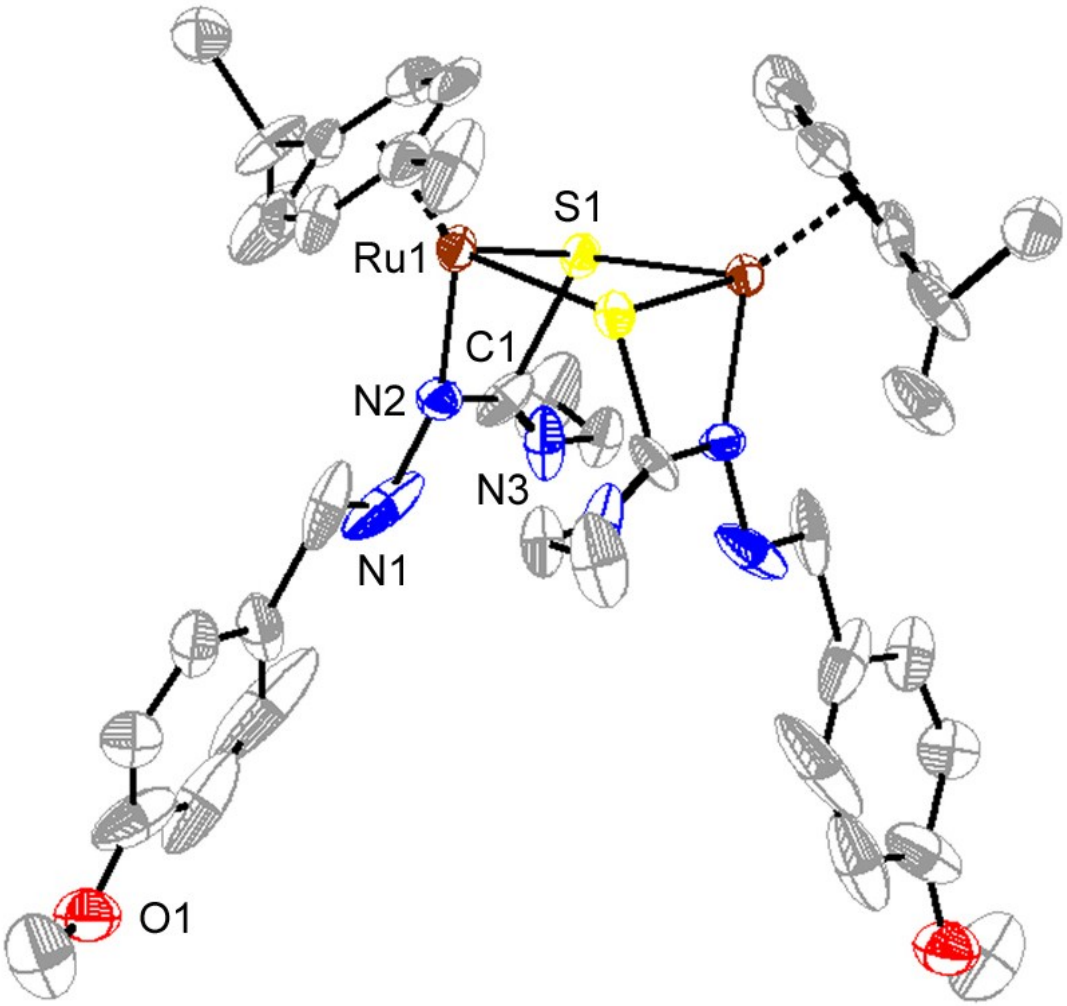

Fig. S5. ORTEP plots of **10**, the H atoms and anions have been omitted for clarity.

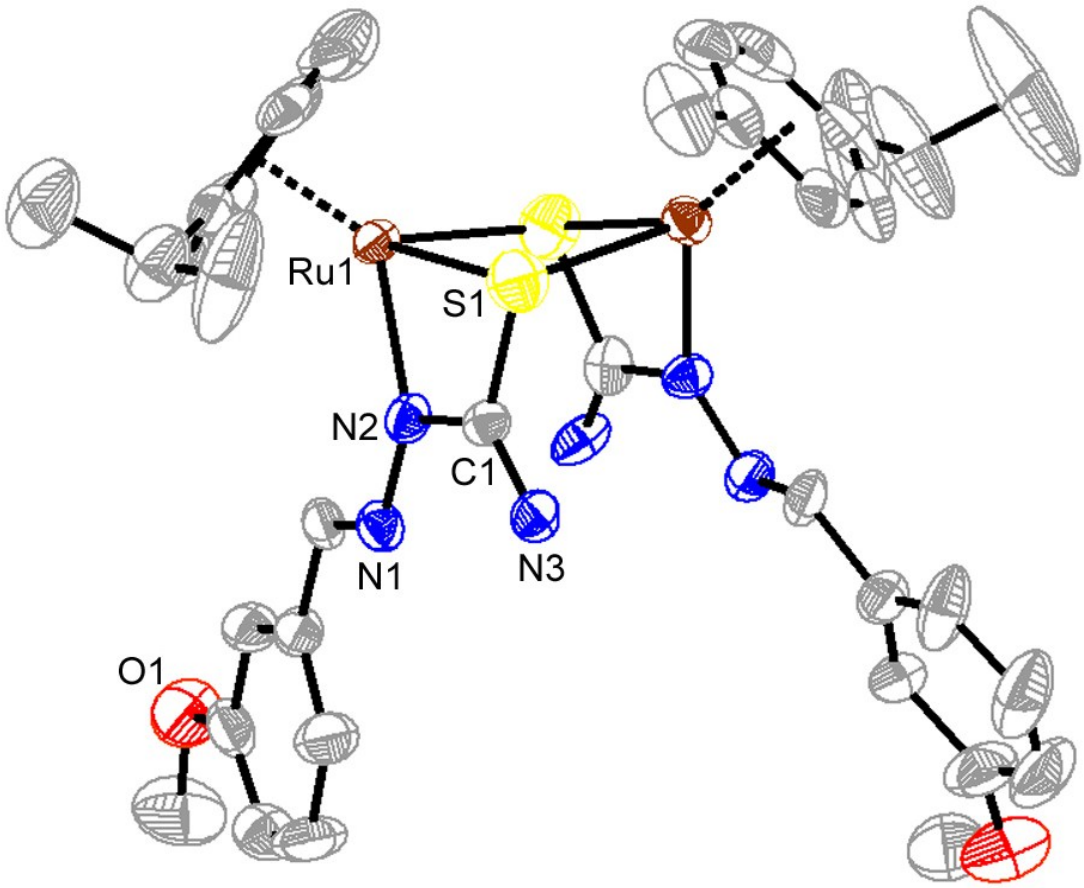

Fig. S6. ORTEP plots of **11**, the H atoms and anions have been omitted for clarity.

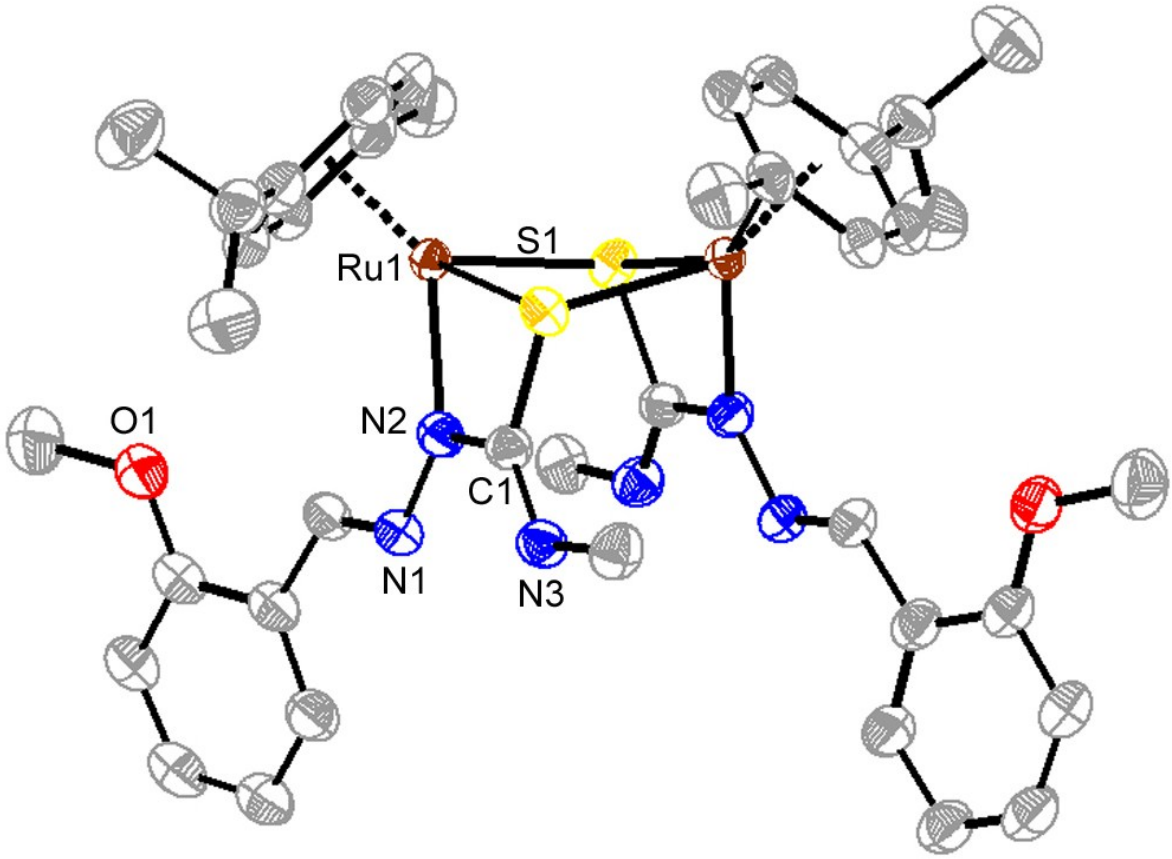

Fig. S7. ORTEP plots of **13**, the H atoms and anions have been omitted for clarity.

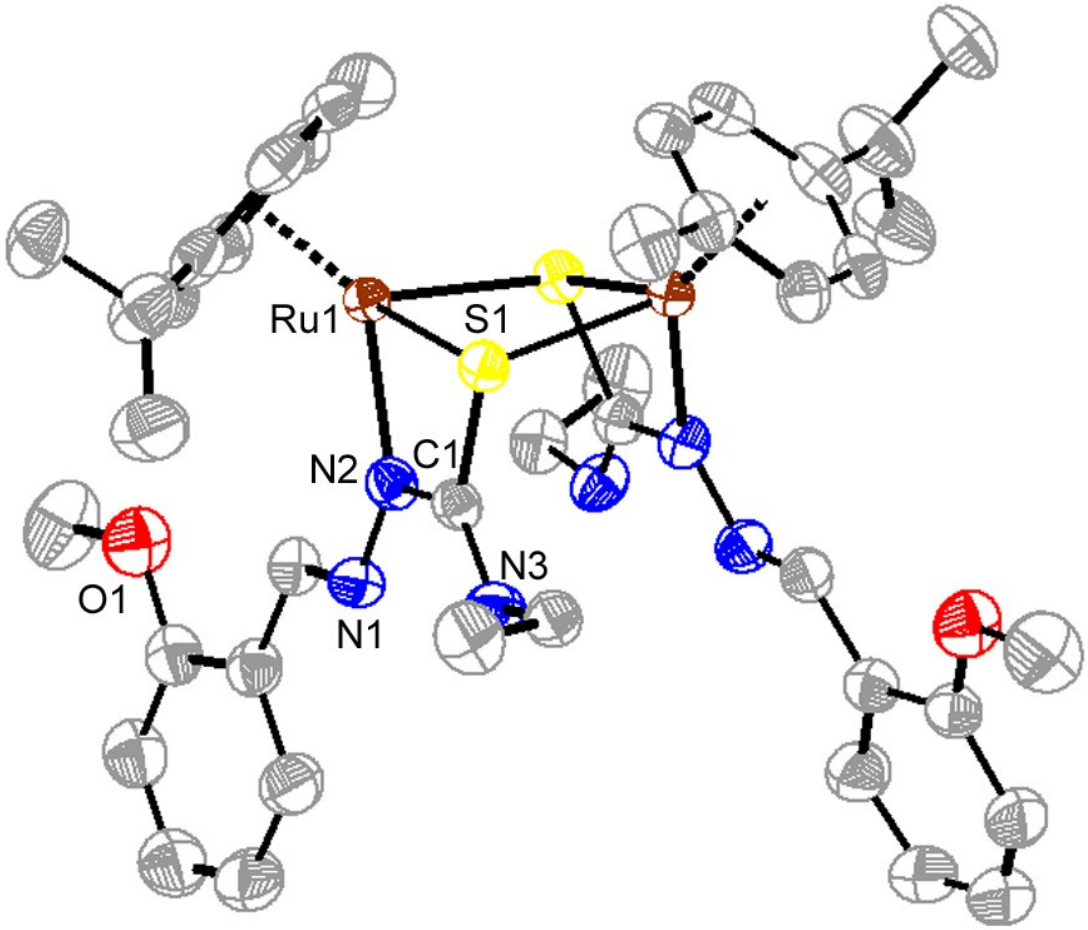

Fig. S8. ORTEP plots of **14**, the H atoms and anions have been omitted for clarity.

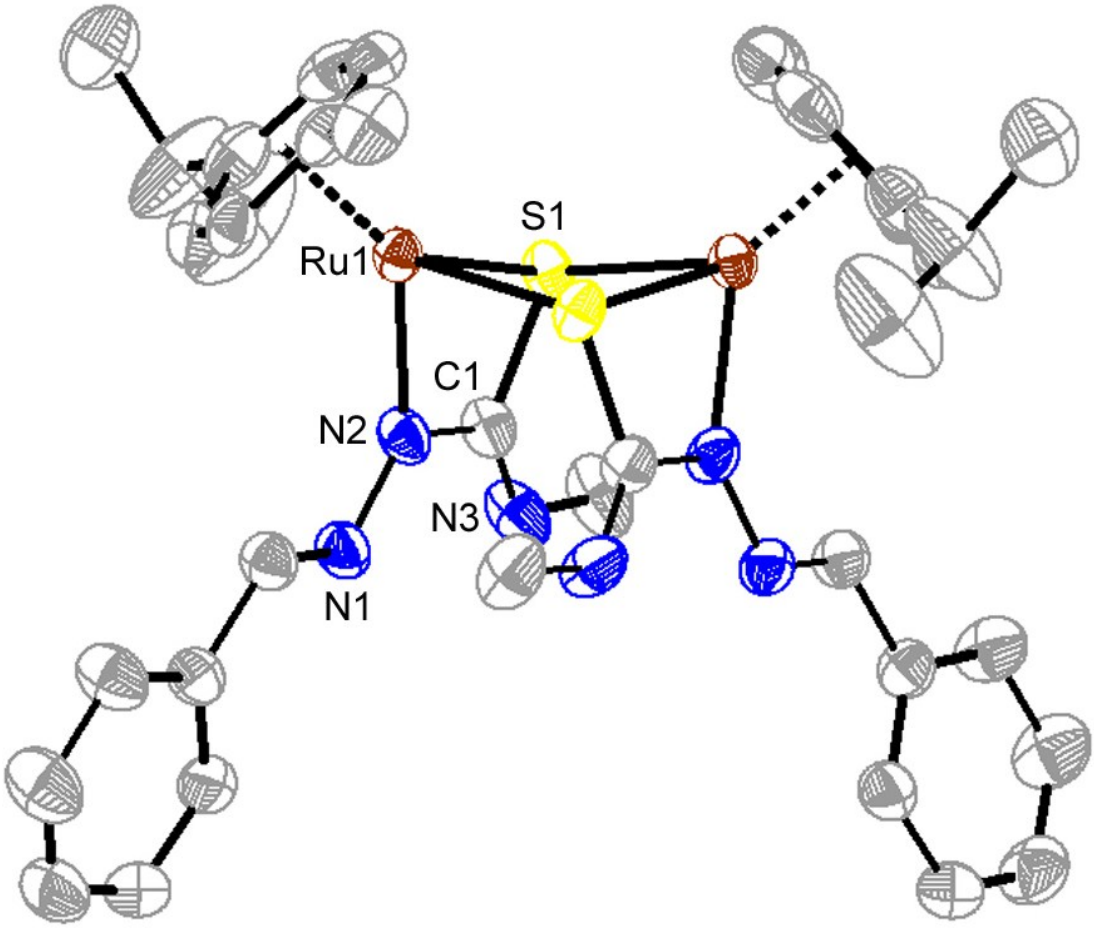

Fig. S9. ORTEP plots of **15**, the H atoms and anions have been omitted for clarity.

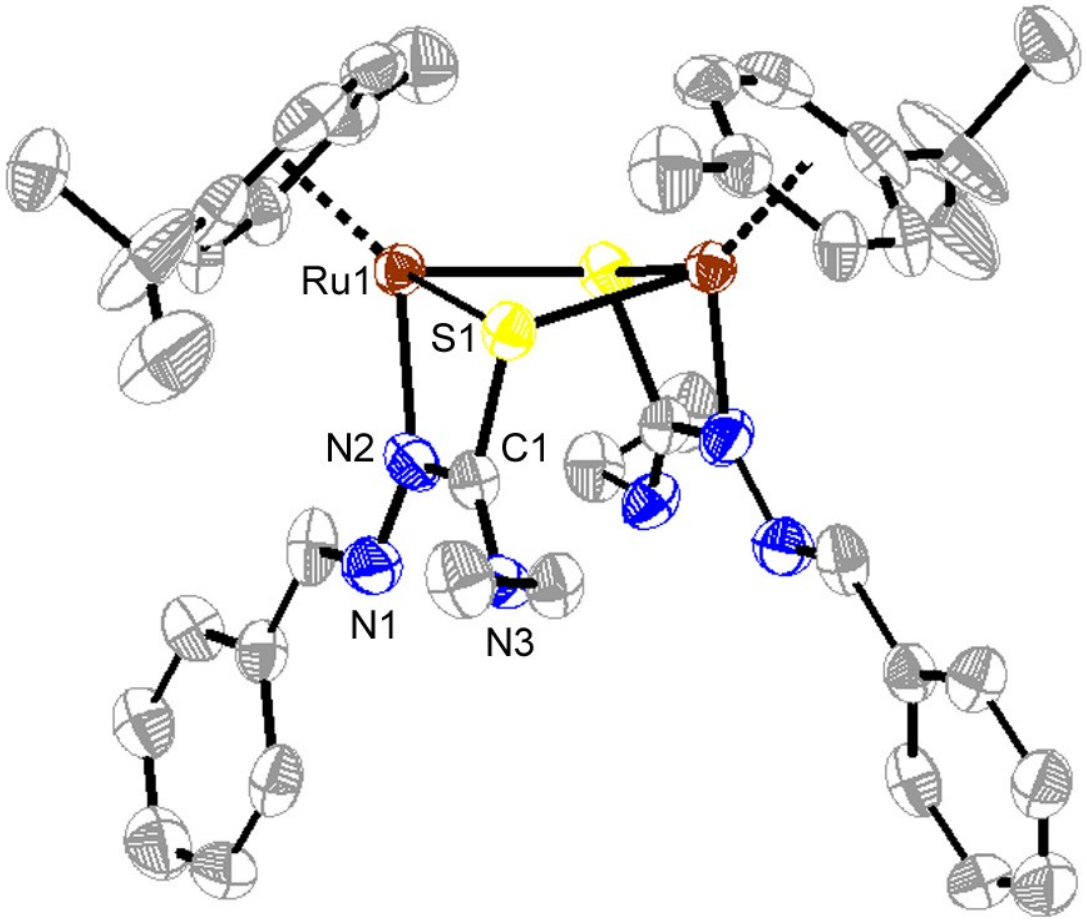

Fig. S10. ORTEP plots of **16**, the H atoms and anions have been omitted for clarity.

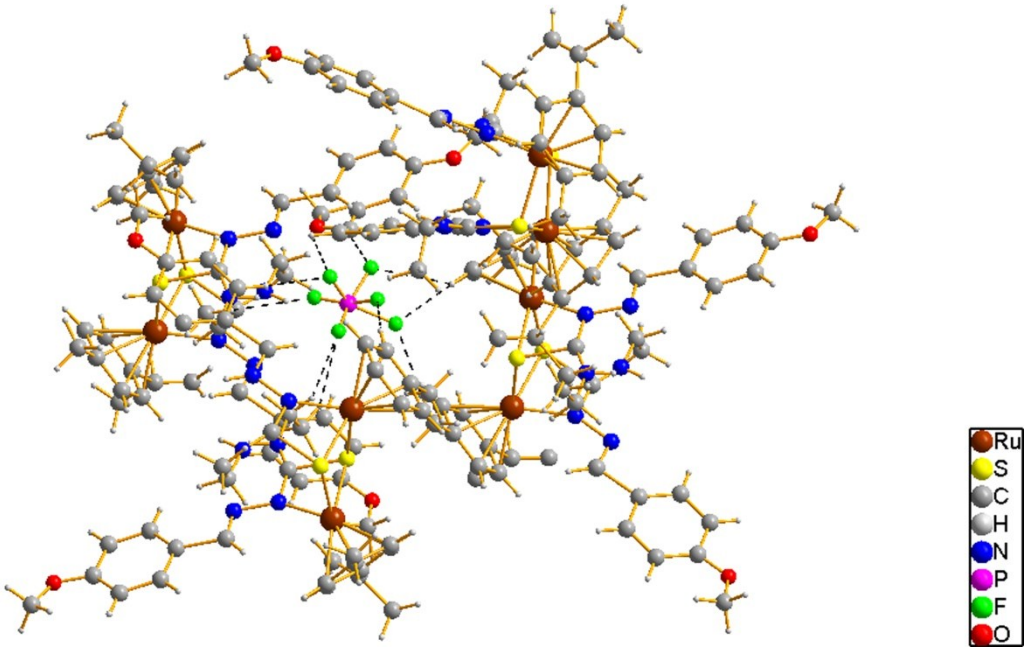

Fig. S11. Packing arrangement and hydrogen bonding for **10.**

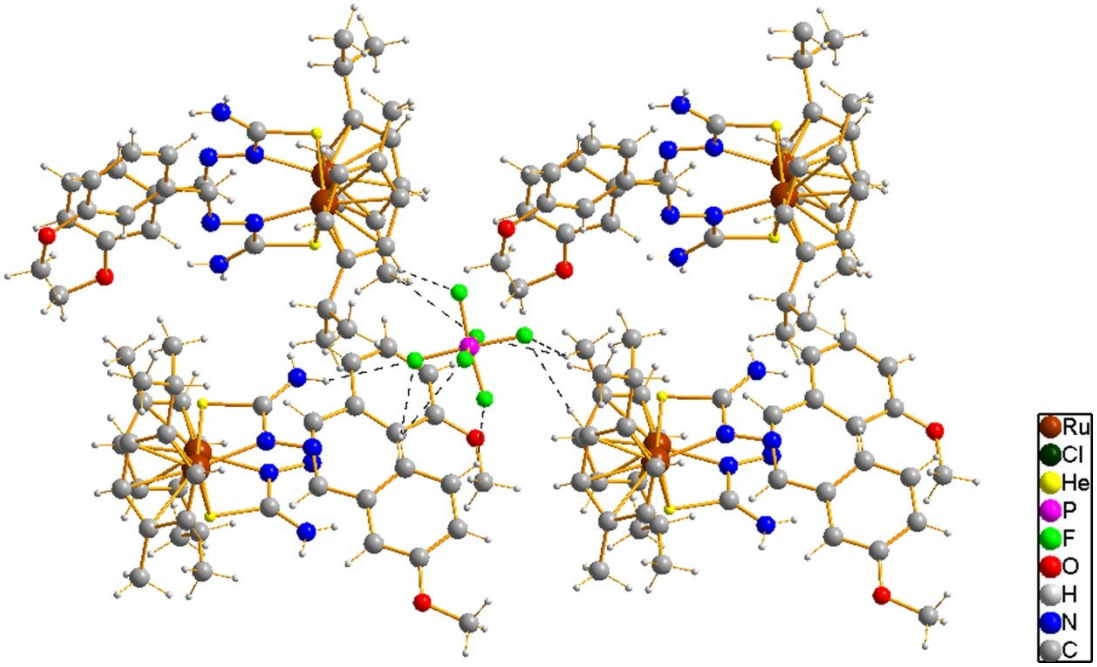

Fig. S12. Packing arrangement and hydrogen bonding for **11.**

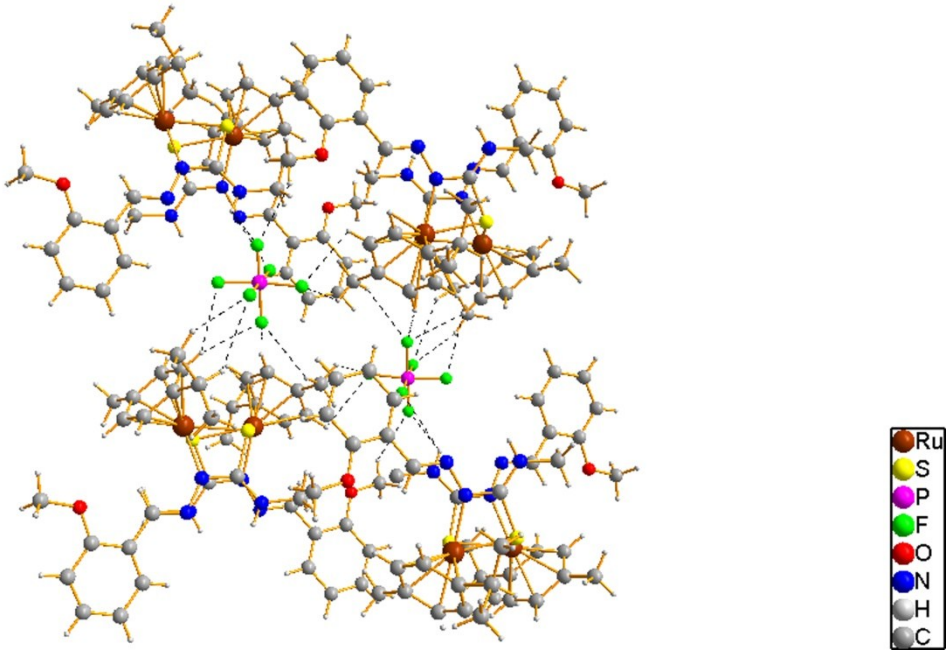

Fig. S13. Packing arrangement and hydrogen bonding for **13.**

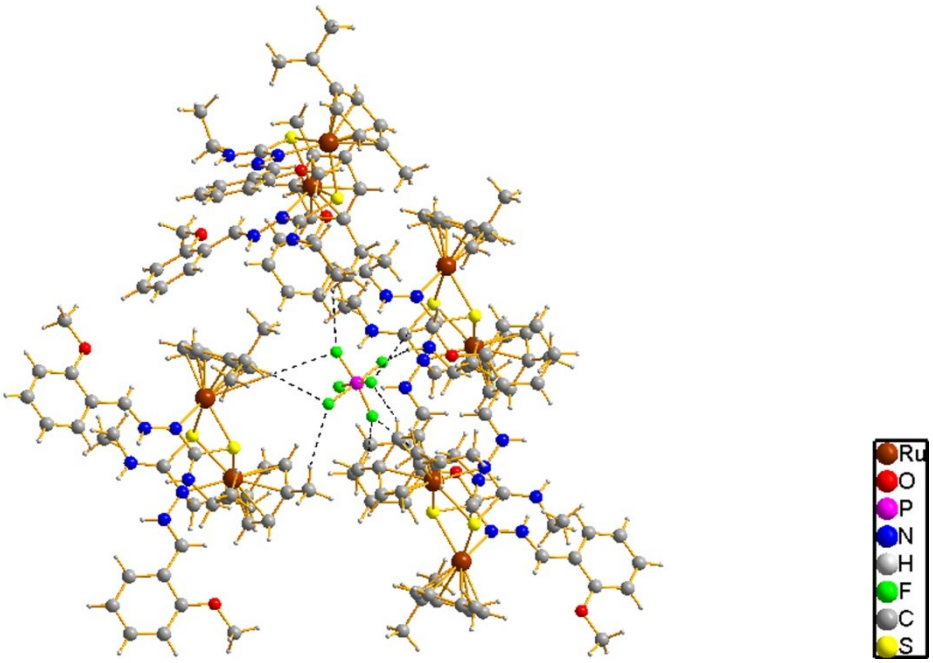

Fig. S14. Packing arrangement and hydrogen bonding for **14.**

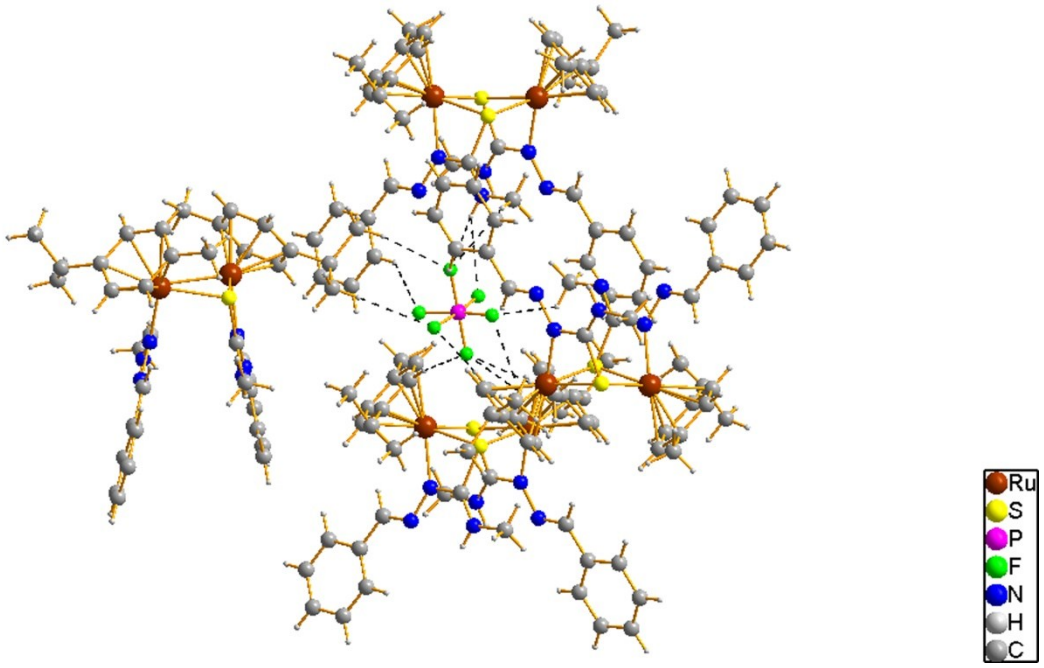

Fig. S15. Packing arrangement and hydrogen bonding for **15.**

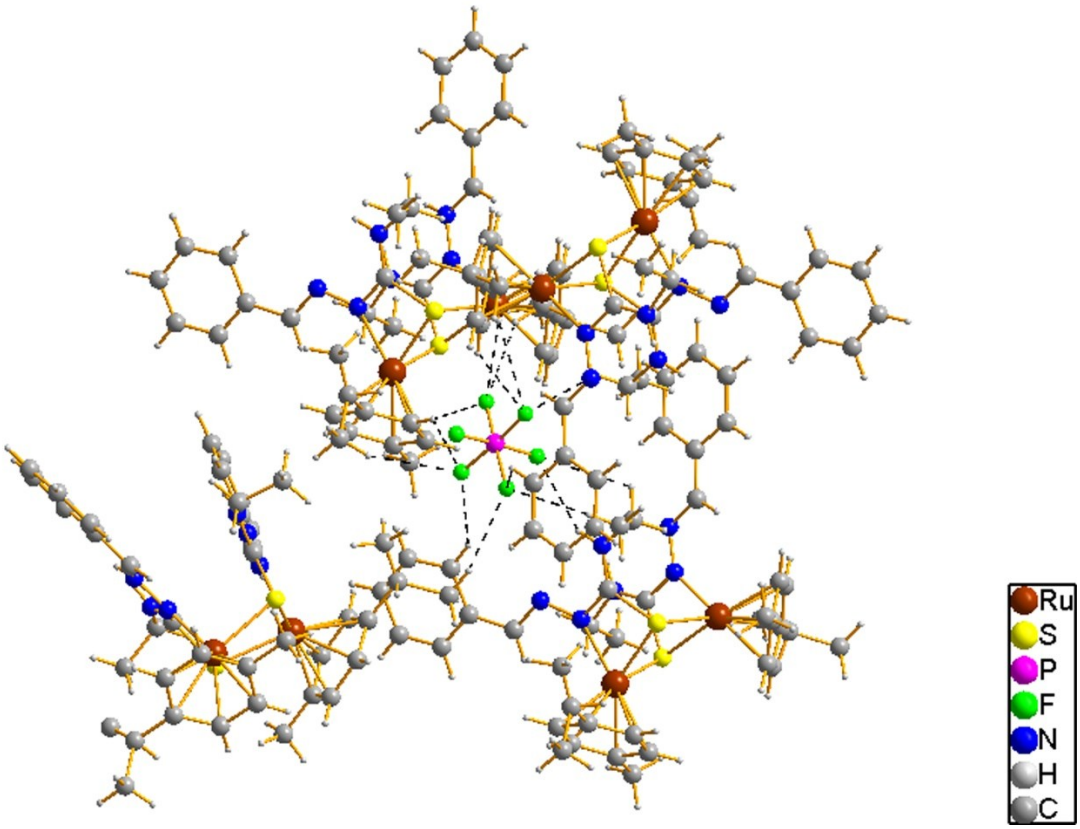

Fig. S16. Packing arrangement and hydrogen bonding for **16.**

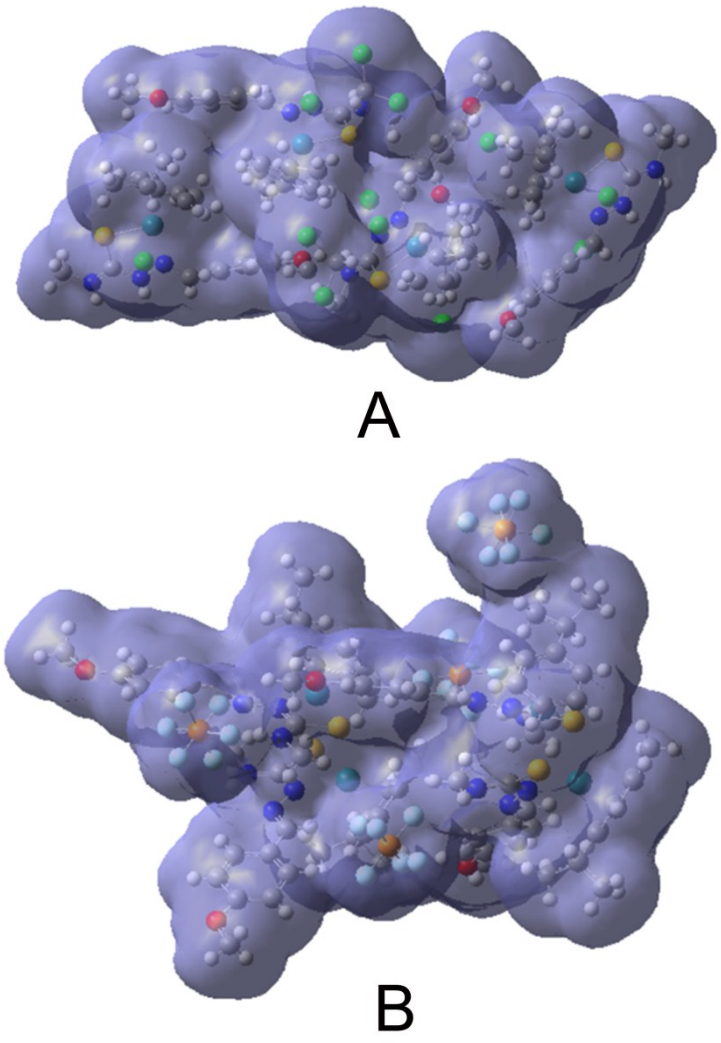

Figure S17. LOL surface of **1** (A) and **9** (B) with isovalue 0.03.

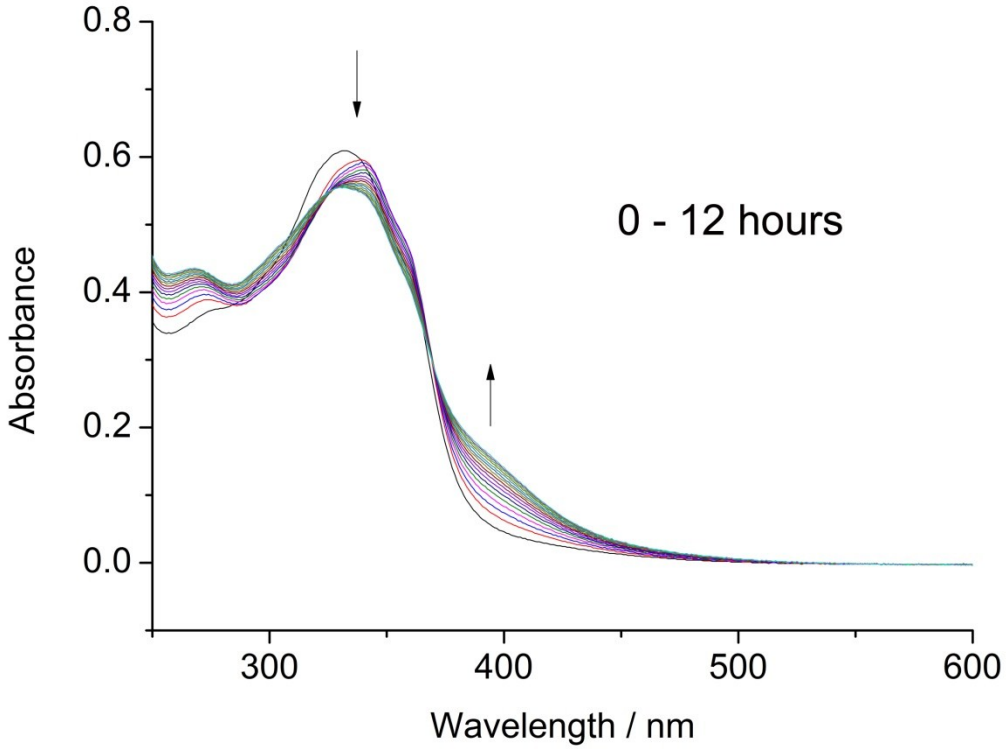

Fig. S18. Time-dependent UV–Vis absorption spectra of **2** measured in DMSO/H_2O.

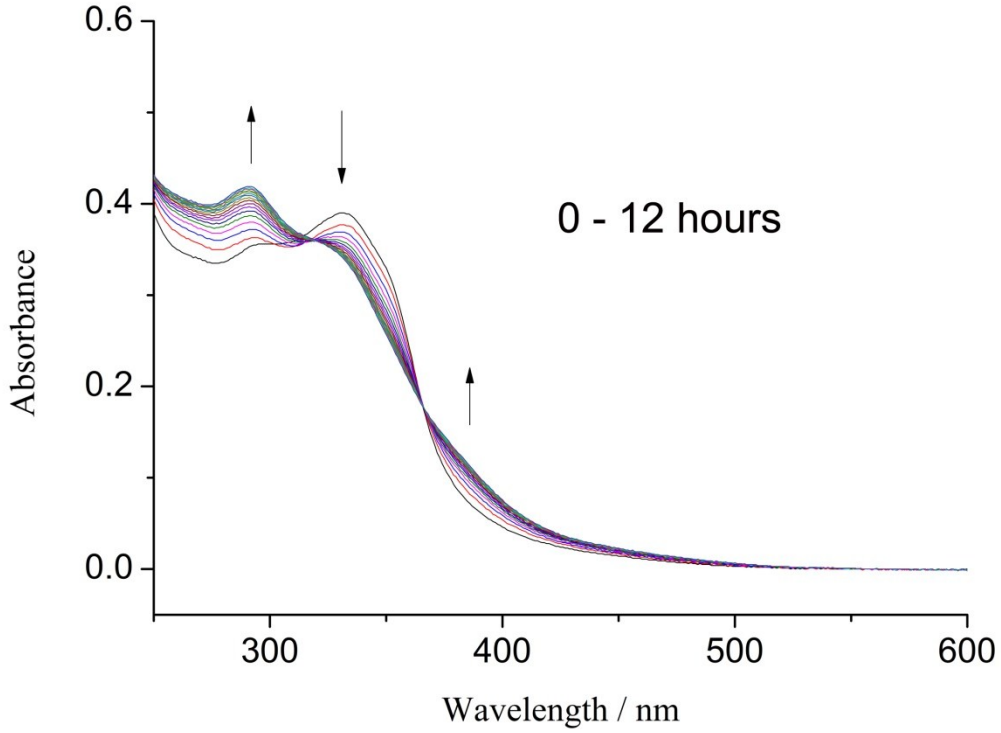

Fig. S19. Time-dependent UV–Vis absorption spectra of **3** measured in DMSO/H_2O.

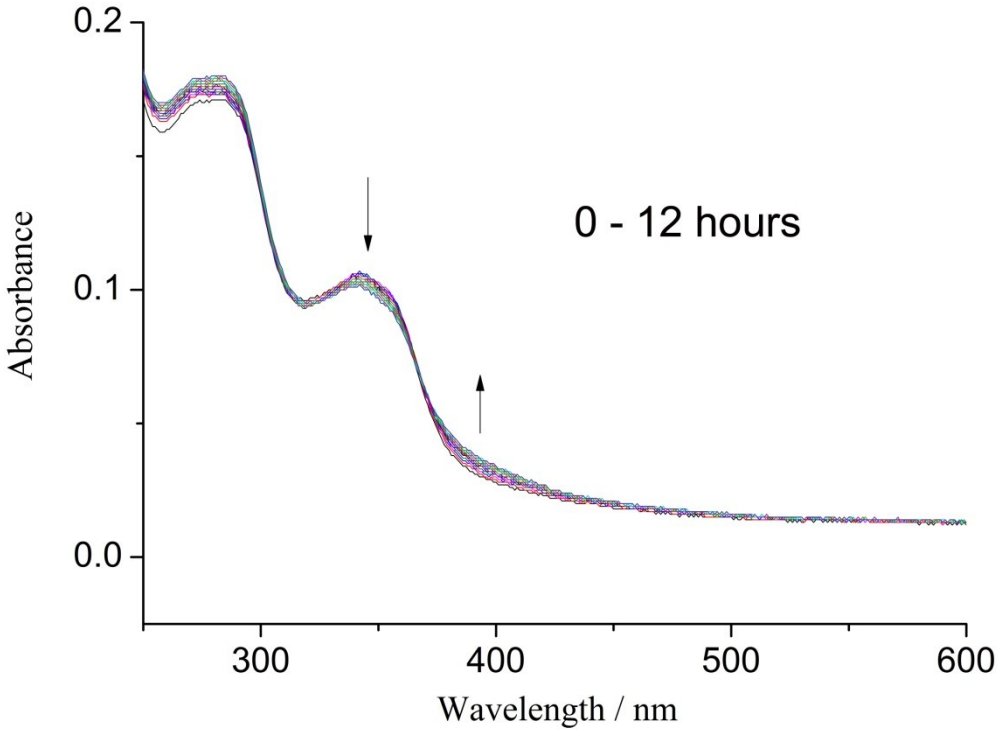

Fig. S20. Time-dependent UV–Vis absorption spectra of **4** measured in DMSO/H_2O.

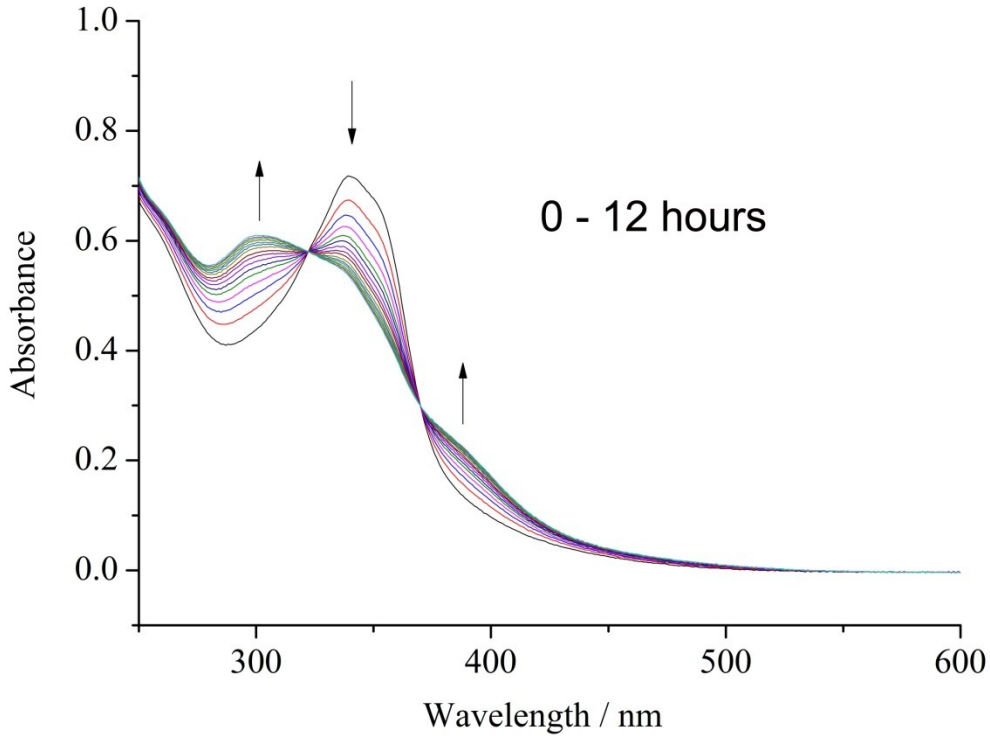

Fig. S21. Time-dependent UV–Vis absorption spectra of **5** measured in DMSO/H_2O.

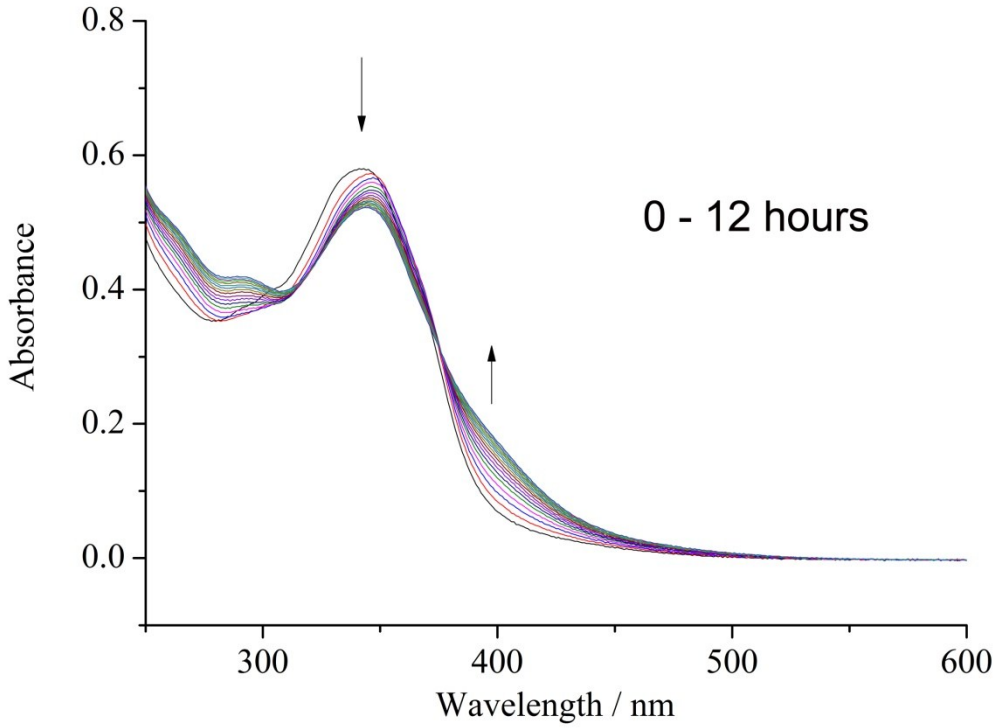

Fig. S22. Time-dependent UV–Vis absorption spectra of **6** measured in DMSO/H_2O.

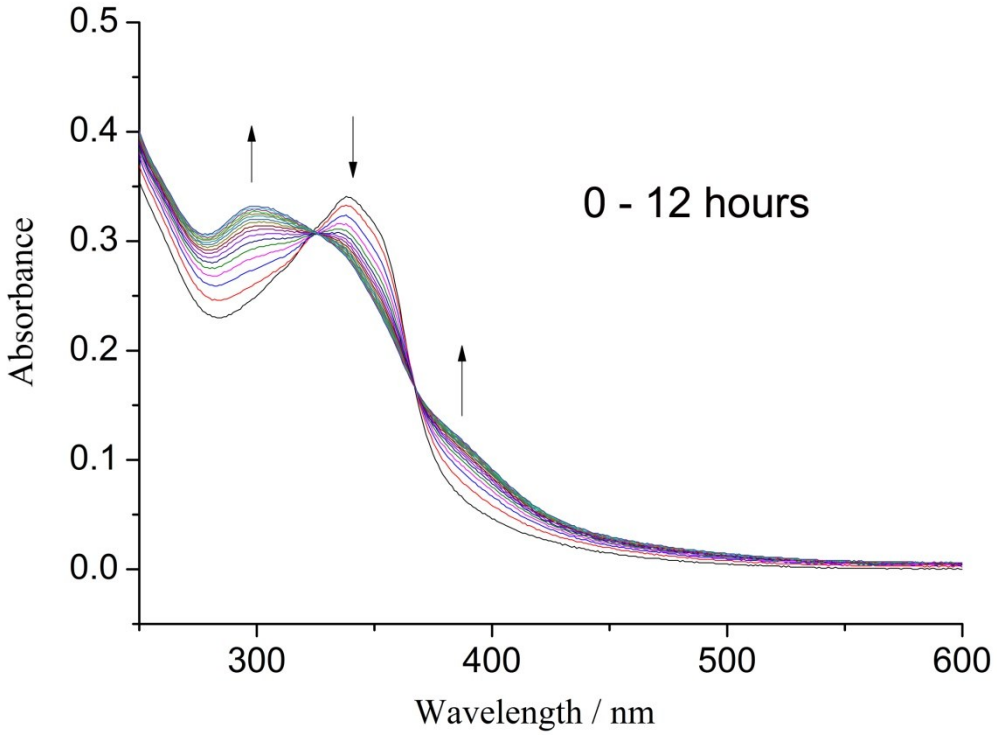

Fig. S23. Time-dependent UV–Vis absorption spectra of **7** measured in DMSO/H_2O.

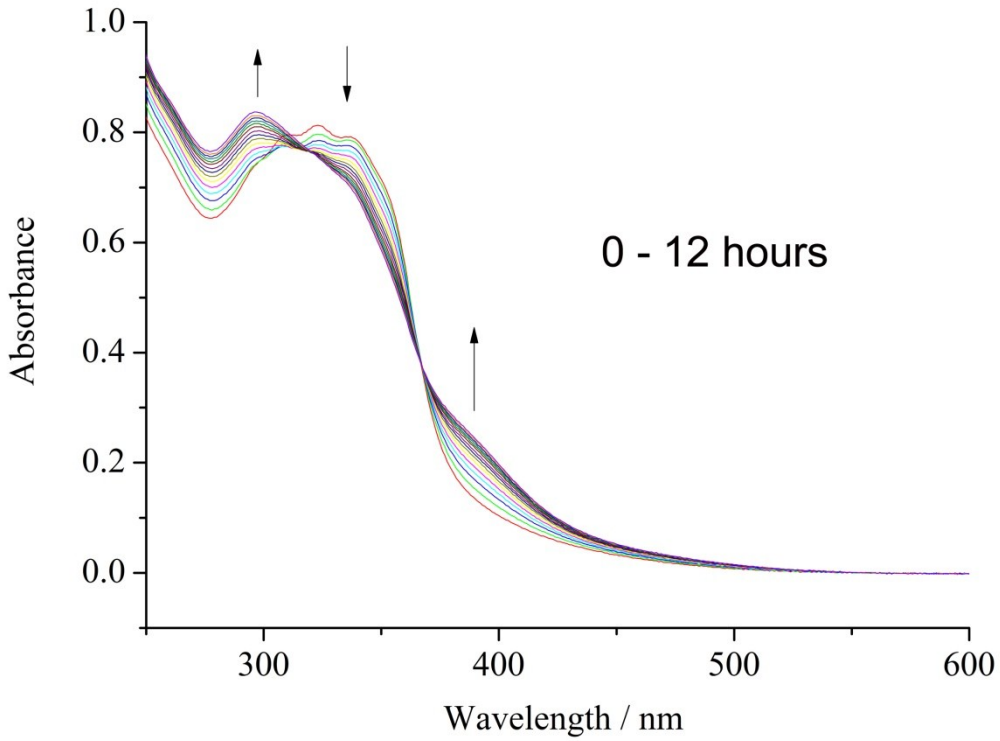

Fig. S24. Time-dependent UV–Vis absorption spectra of **8** measured in DMSO/H_2O.

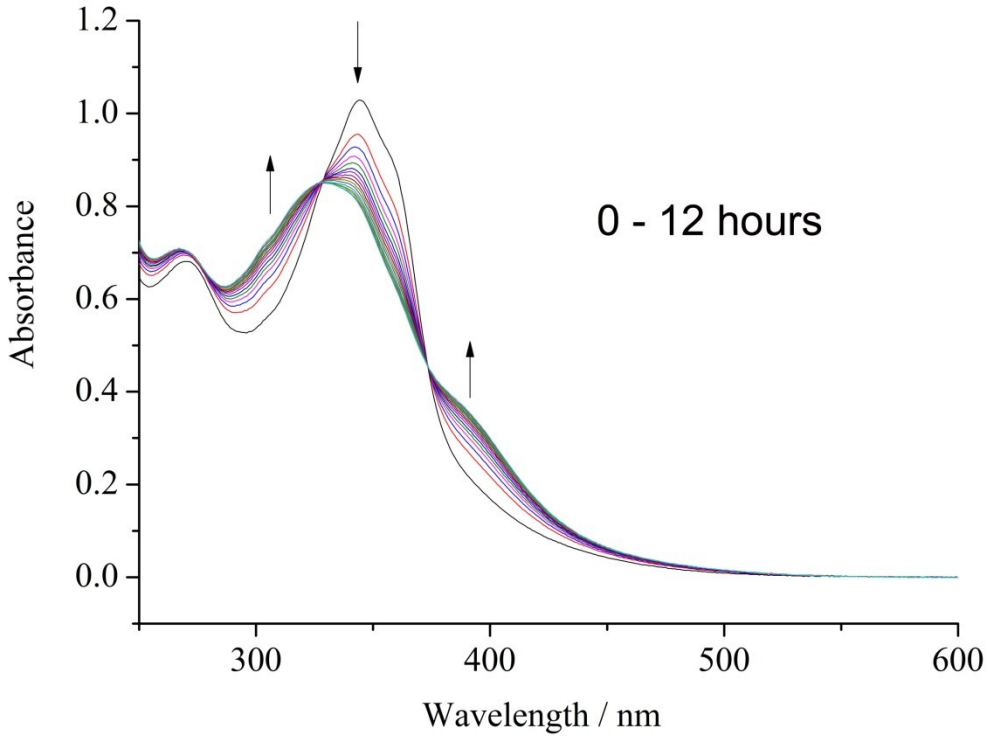

Fig. S25. Time-dependent UV–Vis absorption spectra of **10** measured in DMSO/H_2O.

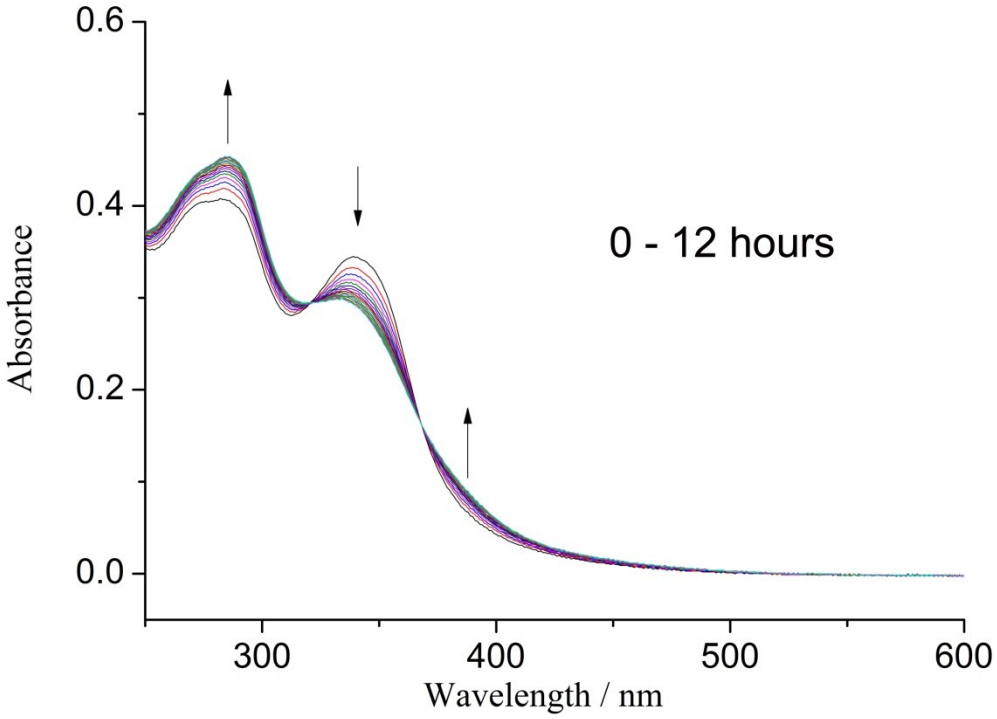

Fig. S26. Time-dependent UV–Vis absorption spectra of **11** measured in DMSO/H_2O.

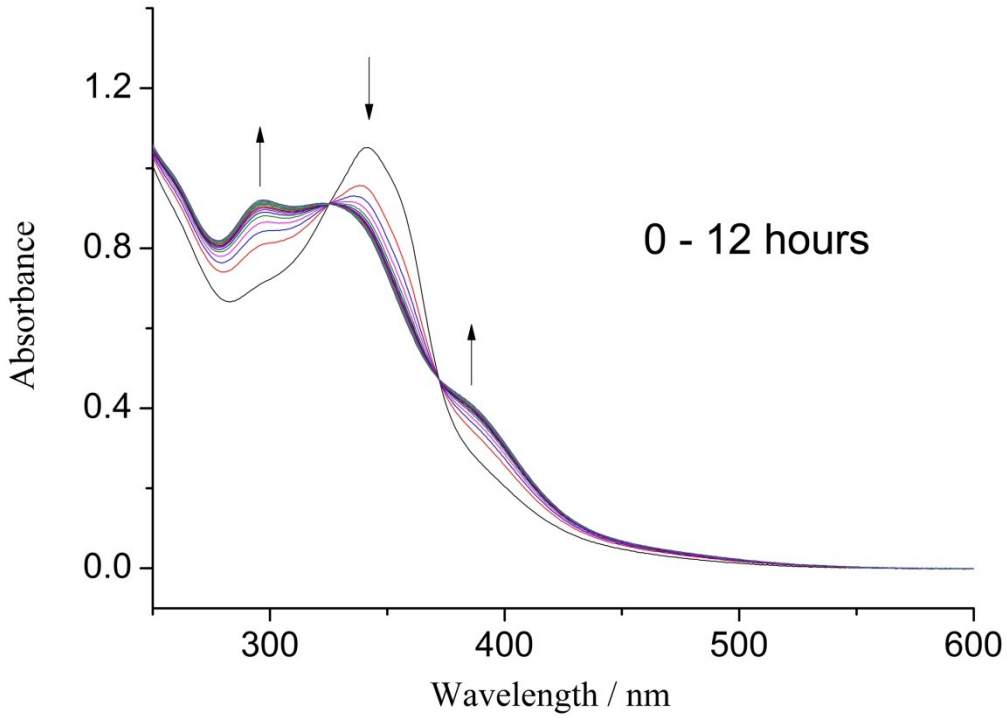

Fig. S27. Time-dependent UV–Vis absorption spectra of **12** measured in DMSO/H_2O.

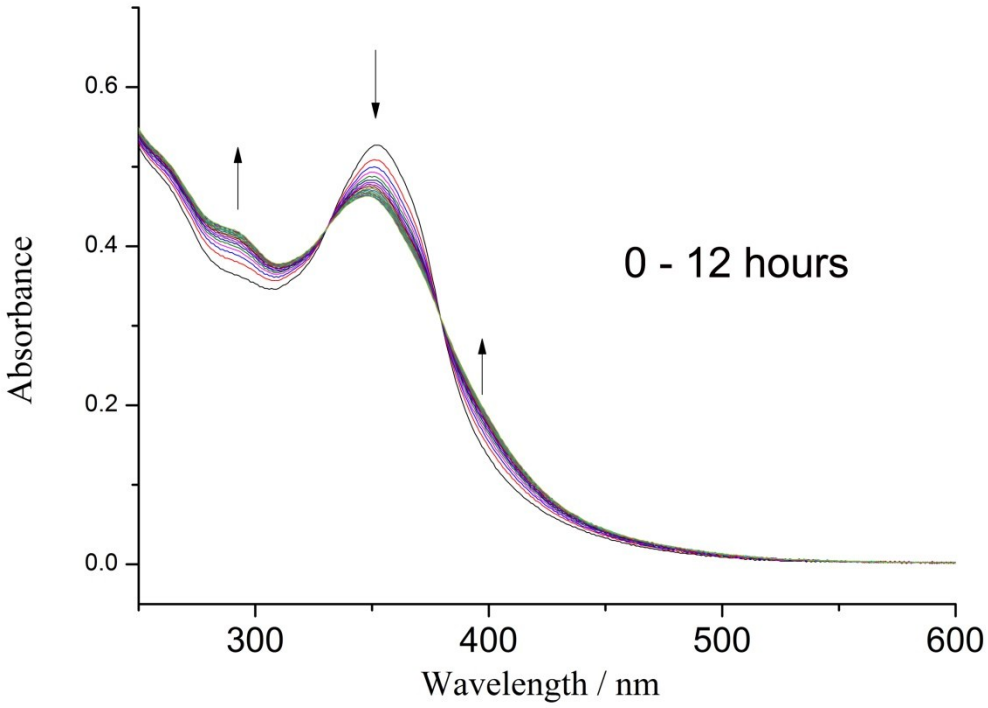

Fig. S28. Time-dependent UV–Vis absorption spectra of **13** measured in DMSO/H_2O.

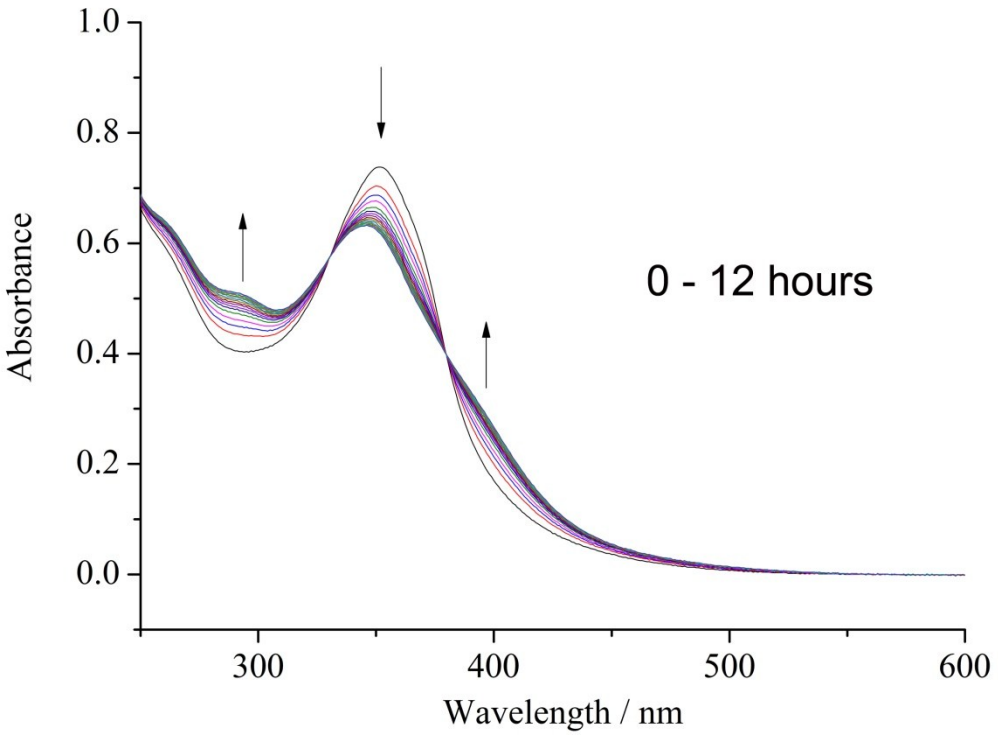

Fig. S29. Time-dependent UV–Vis absorption spectra of **14** measured in DMSO/H_2O.

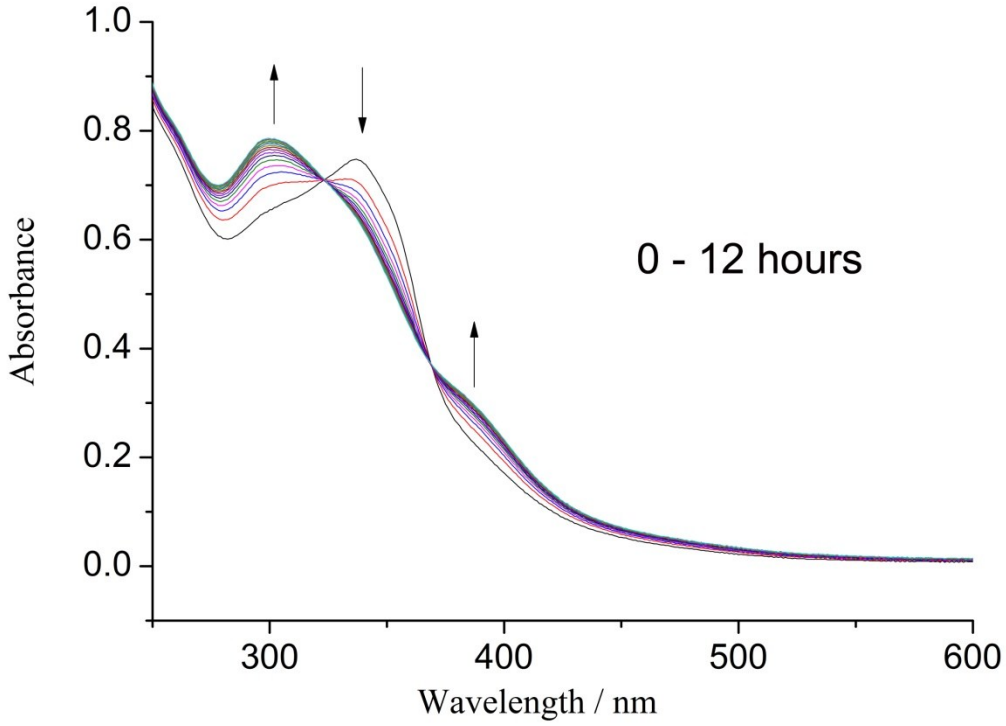

Fig. S30. Time-dependent UV–Vis absorption spectra of **15** measured in DMSO/H_2O.

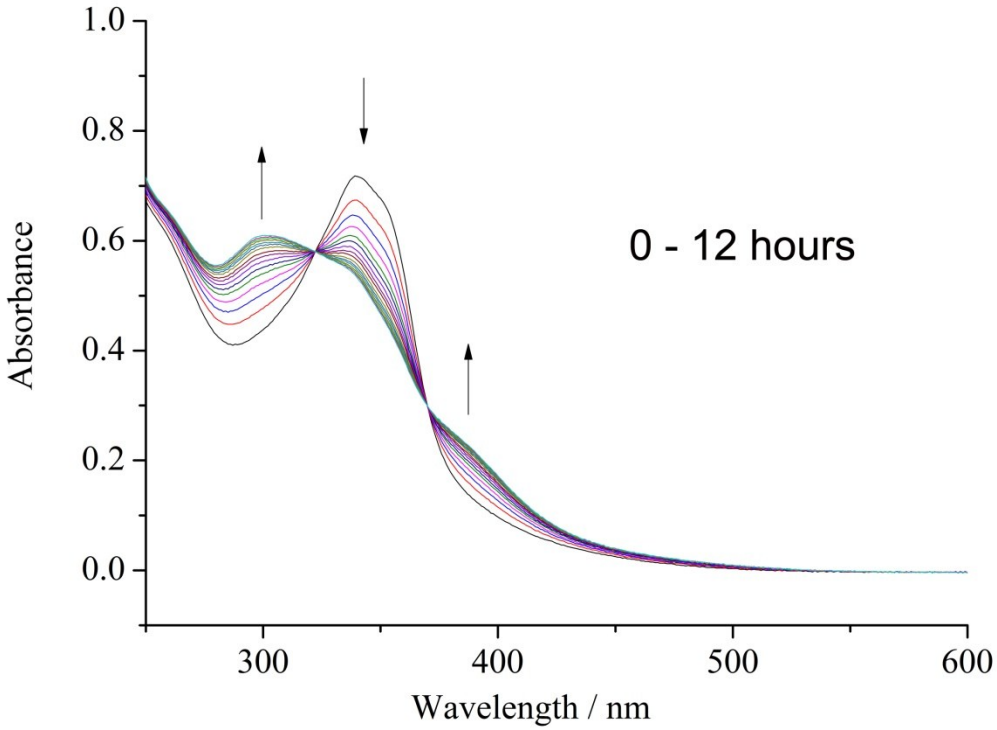

Fig. S31. Time-dependent UV–Vis absorption spectra of **16** measured in DMSO/H_2O.

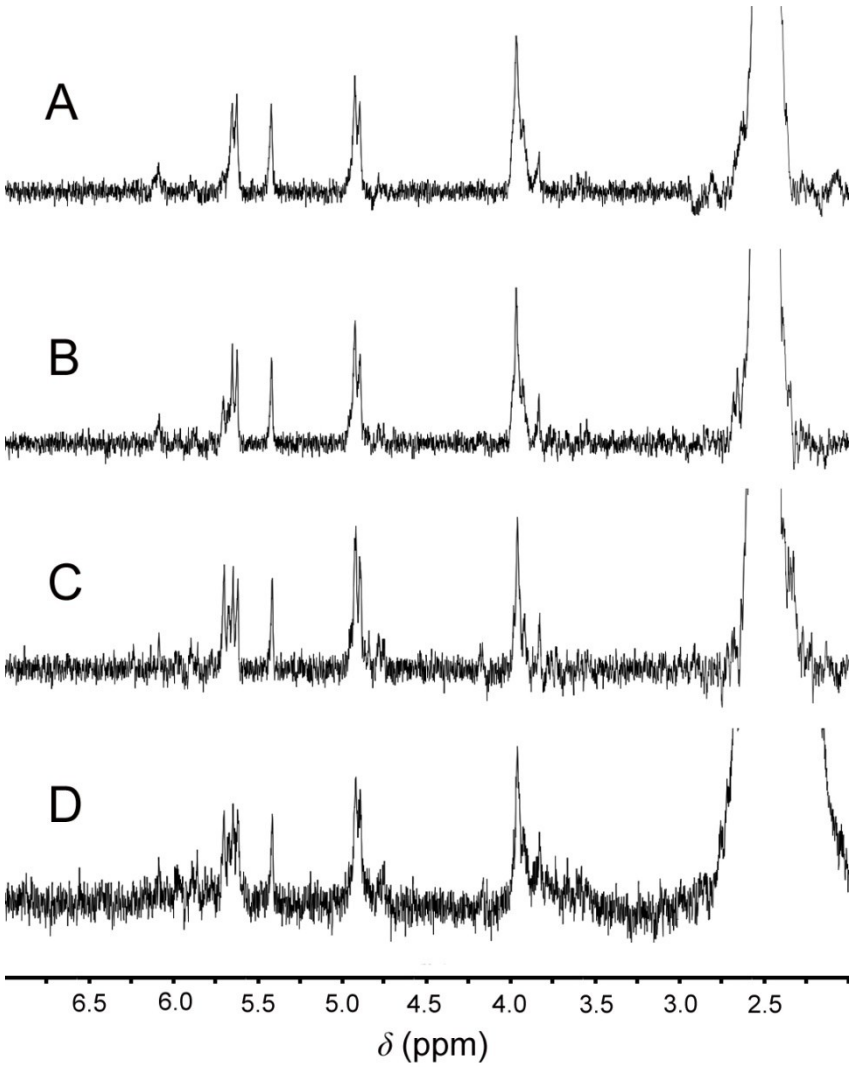

Fig. S32. Downfield region of the ^{1}H NMR spectrum of **9** in DMSO-d_6/D_2O immediately after dissolution (A), 2 h (B), 12 h (C) and 24 h (D).

Table S1. Mayer bond order of **1** and **9** calculated at B3LYP/[SDD (for Ru)/6-311G* (for other atoms)] level..

	1	Mayer Bond Order		**9**	Mayer Bond Order
Ru1-centroid	1.6965(1)	0.313（average）	Ru1-centroid	1.6815(12)	0.286
			Ru1'-centroid	1.6761(16)	0.267
Ru1-S1	2.3559(1)	0.474	Ru1-S1	2.4252(44)	0.346
			Ru1-S1'	2.4222(44)	0.631
Ru1-Cl	2.4154(2)	0.686	Ru1'-S1	2.4129(46)	0.381
			Ru1'-S1	2.4270(46)	0.577
Ru1-N1	2.1318(2)	0.288	Ru1-N2	2.1070(1)	0.230
			Ru1'-N2'	2.1287(1)	0.204
C1-N2	1.3399(1)	1.119	C1-N2	1.3159(2)	1.427
			C1'-N2'	1.3193(2)	1.467
C1-S1	1.6812(2)	1.386	C1-S1	1.7893(2)	1.030
			C1'-S1'	1.7777(2)	1.074
N1-N2	1.3926(1)	0.983	N1-N2	1.4272(2)	1.080
			N1'-N2'	1.3958(2)	1.034
N2−H···Cl2	2.2749(7)	0.225	N−H···F	2.6293(1)	0.015
C2−H···Cl2	2.7356(6)	0.050	C−H···F	2.4008(1)	0.222
			N−H···F	2.3200(2)	0.039
			C−H···F	2.5032(3)	0.024
			C−H···F	2.8053(1)	0.004
			C−H···F	2.5856(2)	0.015
			C−H···F	2.9819(1)	0.018
			C−H···F	2.7959(2)	0.025
			C−H···F	2.6555(4)	0.024
			C−H···F	2.4225(1)	0.065
			C−H···F	2.7530(2)	0.053
			C−H···F	2.6145(1)	0.042
			C−H···F	2.7549(0)	0.022
			C−H···F	2.6334(1)	0.004
			C−H···F	2.5309(3)	0.060
			C−H···F	2.6948(1)	0.044
			C−H···F	2.8944(2)	0.025
			C−H···F	2.8460(1)	0.006